Bull. Mater. Sci., Vol. 18, No. 3, June 1995, pp. 237–246. © Printed in India.

An analysis of the electrical conductivity in $BaSO_4$-added Ag_2SO_4 solid electrolyte system

K SINGH, S M PANDE* and S S BHOGA +
Department of Physics, Nagpur University, Nagpur 440 010, India
*Department of Applied Physics, Ramdeobaba Kamala Nehru College of Engineering, Nagpur 440 013, India
+ Department of Physics, Hislop College, Nagpur 440 001, India

MS received 22 December 1994; revised 20 April 1995

Abstract. The compositions $(1-x)Ag_2SO_4$–$(x)BaSO_4$, where $x = 0{\cdot}01$ to $0{\cdot}6$, were prepared by slow cooling of the melt. The extent of the solid solubility of Ba^{2+} in Ag_2SO_4 was determined by X-ray powder diffraction and scanning electron microscopy. The bulk conductivity of each sample was obtained using a detailed impedance analysis. The partial substitution of Ba^{2+} results in the enhancement of conductivity in compliance with the classical aliovalent doping theory. A simplistic model based on lattice distortion (expansion) due to partial substitution of Ag^+ by the bigger Ba^{2+} has been considered to explain enhanced conductivity. Beyond solid-solubility limit (5·27 mole%) the $BaSO_4$-dispersed Ag_2SO_4 conductivity follows the usual trend seen in binary systems. An increase in conductivity in this case is discussed in the light of interfacial reactions and surface defect chemistry. The maximum conductivity in 20 mole% $BaSO_4$ dispersed Ag_2SO_4 is due to percolation threshold.

Keywords. Solid solubility; ionic radius; lattice distortion; space charge; ionic conductivity.

1. Introduction

The sulphate-based solid electrolytes differ in some respect from other solid electrolyte materials in the sense that they are thermodynamically more stable, less expensive and easy to handle. An advantage is that many monovalent and divalent cations have high mobility in their high-temperature phases and the choice of electrode materials is greater in electrochemical applications in general (Heed *et al* 1975). Particularly, they have potential applications in SO_x galvanic gas sensors (Gauthier and Chamberland 1977; Liu *et al* 1990).

Among others, silver sulphate has received little attention. It is a polymorphic compound with two different modifications which are β-phase (orthorhombic) below 416°C and α-phase (hexagonal) above this temperature. The low- and high-temperature phases of Ag_2SO_4 are isomorphous to those of $BaSO_4$.

Several attempts have been made to enhance the ionic conductivity in polycrystalline solids. In this direction essentially the following approaches have been adopted: (i) aliovalent substitution of conducting cations (Hofer *et al* 1981), (ii) opening of the lattice structure by substitution with wrong size ion (Singh and Bhoga 1992), (iii) optimization of the preparative parameters (Singh and Deshpande 1982), (iv) trapping of high-temperature highly conducting phases at room temperature (Singh *et al* 1988), (v) stabilization of open-channel structure (Rodger *et al* 1985), and (vi) dispersion of insoluble second phase (Liang 1973). The first two approaches have been important not only from the point of development of electrolytes but also for basic understanding.

The conductivity is strongly correlated to the vacancy concentration regardless of the size and the electronic configuration of the substituting ions (Hofer *et al* 1981). However, dependence of conductivity on aliovalent ionic size and charge has been reported (Singh 1988; Singh and Bhoga 1992). A decrease in conductivity due to partial substitution as well as dispersion of $CaSO_4$ has been reported earlier (Singh *et al* 1995). We have introduced the concept of lattice contraction (due to the partial replacement of host by smaller-size guest cation) to understand the fall in conductivity. The present investigation has been undertaken to probe further into the role of ionic size of aliovalent cation on the ionic conductivity. A partial substitution of Ag^+ by Ba^{2+} has been made with a view to distort the lattice while creating extrinsic vacancies on the basis of the following formula:

$$Ag_{2-2x}Ba_x\square_xSO_4.$$

A few biphase mixtures of Ag_2SO_4 with $BaSO_4$ have also been investigated with a view to seeing the effect of valency and ionic size in space charge region.

2. Experimental

The initial ingredients Ag_2SO_4 and $BaSO_4$ with purity greater than 99% were procured from E Merck, India. Appropriate mole fractions of the above chemicals in $(1-x)Ag_2SO_4$–$(x)BaSO_4$ ($x = 0{\cdot}01$ to $0{\cdot}6$) were prepared by slow-cooling the melt in silica ampoules at a predetermined cooling rate of 1·5°C/min. The prepared samples were characterized by X-ray powder diffraction and scanning electron microscopy as discussed elsewhere (Singh *et al* 1995).

For electrical conductivity measurements, the samples were obtained in the form of circular discs of 9 mm dia and 2 mm thickness by pressing the powder in a Specac (US) stainless steel die-punch and hydraulic press. A good ohmic contact was ensured by using quality graphite paint (Eleteck, India) followed by baking at 200°C for 1 h. The above process was carried out in a dark room. The pellets were sintered at 450°C for 24 h before spring-loading them between silver electrodes of a sample holder. Prior to impedance measurements, the spring-loaded sample was again heated to 360°C for 2 h in order to homogenize the charge carriers in the sample and simultaneously to remove the moisture content therein. The AC electrical conductivity was measured as a function of frequency in the range 5 Hz to 13 MHz and temperature in the range 450 to 250°C using a HP 4192A LF impedance analyser. HP 16048 test leads were used for electrical connections from sample to analyser to avoid any otherwise parasitic impedance due to improper connecting cables. The temperature of the furnace was controlled to ± 1°C using a Eurotherm 810 PID temperature controller. The entire measurement system was properly shielded. The reproducibility of impedance data was confirmed by repeating the measurement on freshly prepared samples.

3. Results and discussion

Table 1 shows the experimental d and relative intensity I/I_0 values for $(1-x)Ag_2SO_4$–$(x)BaSO_4$ (where $x = 0{\cdot}000$, $0{\cdot}0527$ and $0{\cdot}0757$) along with the JCPDS data of parent phases. It is worth noting that in the X-ray diffraction pattern

Table 1. A comparison of d and I/I_0 with JCPDS data for $(1-x)Ag_2SO_4$–$(x)BaSO_4$ ($x = 0{\cdot}00$, $0{\cdot}0527$ and $0{\cdot}0757$).

Ag_2SO_4 ($x = 0{\cdot}00$)		$x = 0{\cdot}0527$		$x = 0{\cdot}0757$		*JCPDS		Phase (hkl)
d	I/I_0	d	I/I_0	d	I/I_0	d	I/I_0	
4·670	5	4·711	9	4·709	10	4·699	10	Ag(111)
—	—	—	—	4·361	2	4·334	30	Ba(101)
3·969	18	4·018	23	3·999	26	3·994	25	Ag(220)
—	—	—	—	3·444	5	3·445	100	Ba(021)
—	—	—	—	3·318	4	3·319	70	Ba(210)
3·164	92	3·179	50	3·177	93	3·177	70	Ag(040)
2·866	100	2·879	100	2·876	100	2·873	100	Ag(311)
—	—	—	—	2·731	2	2·735	45	Ba(002)
2·636	87	2·652	43	2·645	87	2·644	90	Ag(022)
2·521	19	2·535	16	2·531	18	2·530	17	Ag(202)
2·410	30	2·428	20	2·425	24	2·421	30	Ag(331)
—	—	—	—	2·355	4	2·325	14	Ba(022)
—	—	—	—	2·104	4	2·106	75	Ba(212, 231)
1·973	11	1·978	12	1·979	11	1·980	11	Ag(242)
1·918	35	1·929	21	1·924	29	1·926	30	Ag(351)
—	—	—	—	1·759	3	1·762	8	Ba(103)
—	—	—	—	1·647	3	1·644	3	Ba(151)
—	—	—	—	1·587	5	1·587	4	Ba(421)
1·542	10	1·549	10	1·545	8	1·546	8	Ag(371)
—	—	—	—	1·363	2	1·363	18	Ba(004, 520)

Ag–Ag_2SO_4 (orthorhombic) JCPDS card numbers 27–1403
Ba–$BaSO_4$ (orthorhombic) JCPDS card numbers 24–1035

of sample with $x = 0{\cdot}0527$, not a single line corresponding to $BaSO_4$ is observed, whereas all the experimental lines are found to be in good agreement with the JCPDS data for Ag_2SO_4. The absence of lines corresponding to $BaSO_4$ for this composition indicates the formation of a solid solution. From table 1 it is also evident that when the dopant concentration (x) is increased to $0{\cdot}0757$, a few weak lines corresponding to $BaSO_4$ are observed. The samples with ($x > 0{\cdot}0757$) in general show strong lines corresponding to Ag_2SO_4 and very weak ones for $BaSO_4$. The small deviation in the d values for Ag_2SO_4 can be due to the partial replacement of Ag^+ by the bigger Ba^{2+}, since such a replacement results in local lattice distortions. The lattice cell constants presented in table 2 show that the host Ag_2SO_4 lattice undergoes an expansion upon Ba^{2+} addition within the solid solubility limit. From this study the solid-solubility limit of $BaSO_4$ in Ag_2SO_4 is set up to be 5·27 mole%.

The variations of $\log(\sigma)$ as a parametric function of $BaSO_4$ concentration in high- and low-temperature modifications are shown in figures 1 and 2 respectively. In general, it can be seen that as impurity concentration increases the conductivity also increases and exhibits a maximum within solid-solubility limit in both the phases. Furthermore, in low-temperature modification one more conductivity maximum (figure 2) is observed at 20 mole% $BaSO_4$. The results of low temperature modification are similar to those of earlier reported results in case of Li_2SO_4:$CaSO_4$, AgBr:AgI and Na_2SO_4:Na_2WO_4 (Singh and Bhoga 1990; Dekker

1990; Rao *et al* 1992). In order to discuss the conductivity behaviour of the Ag_2SO_4:$BaSO_4$ system, the investigated compositional range is divided into two regions: region I: $0 \leqslant x \leqslant 0{\cdot}0527$, and region II: $0{\cdot}0527 < x \leqslant 0{\cdot}6$.

3.1 *Region I*

The bulk conductivity of each composition is obtained using a computerized impedance analysis. Figure 3 illustrates the variation of $\log(\sigma T)$ with $10^3/T$ within the solid-solubility range. The break-over in the conductivity indicates the occurrence of transition from orthorhombic to hexagonal phase.

Table 2. A comparison of lattice cell constants of doped and undoped Ag_2SO_4 as calculated from table 1.

Cell constant	$x = 0{\cdot}0$	$x = 0{\cdot}0527$
a(Å)	10·247	10·287
b(Å)	12·688	12·764
c(Å)	05·748	05·765
Cell volume Å^3	747·32	756·96

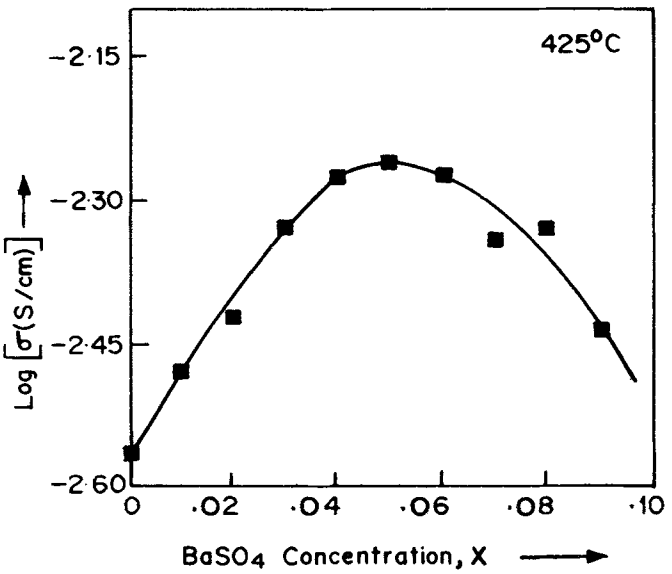

Figure 1. Variation of $\log(\sigma)$ with x in $(1-x)Ag_2SO_4$–$(x)BaSO_4$ in high-temperature phase (at 425°C).

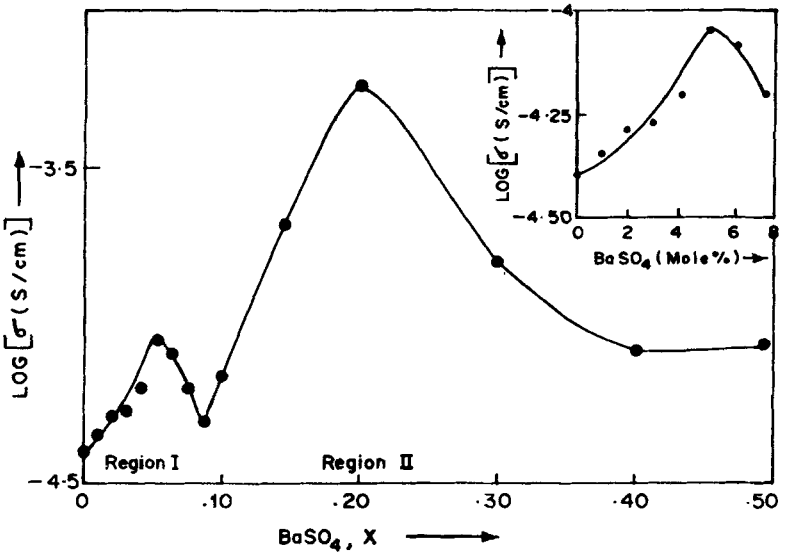

Figure 2. Variation of $\log(\sigma)$ with x in $(1-x)Ag_2SO_4$–$(x)BaSO_4$ in low-temperature phase (at 300°C).

In both ranges of modification of Ag_2SO_4, upon Ba^{2+} addition the conductivity, as expected, increases initially and falls off after attaining a maximum at 5% vacancy (5·27 mole%). The initial rise in conductivity could be understood by considering that the dopant Ba^{2+} occupies an Ag^+ site in the Ag_2SO_4 lattice to produce one Ba_{Ag} and one extrinsic Ag ion vacancy V'_{Ag} in order to maintain the charge neutrality. At low doping levels with increase in Ba^{2+} concentration the conductivity increases as number of vacancies (V'_{Ag}) increases. At higher Ba^{2+} concentration the extrinsic Ag^+ vacancies interact with the dopant ions to form an associate, termed cluster. Such extended clustering of defects hinders the Ag^+ mobility and hence the fall in conductivity. The doping amount of $BaSO_4$ for which defect–defect interactions predominate is greater than 5% vacancy. The results are in excellent agreement with conductivity behaviour vis-a-vis aliovalent doping (Hofer *et al* 1981; Singh and Bhoga 1990; Dekker 1990; Rao *et al* 1992). It is worth noting here that the magnitude of conductivity enhancement in low-temperature modification is more pronounced compared to that in high-temperature hexagonal phase. Obviously, the structure of hexagonal phase is more open, thus the effect of ionic size of the guest cation on the lattice structure is expected to be negligible (Hofer *et al* 1981). In contrast, in low-temperature orthorhombic phase, the ionic size has a predominant role to play from ion mobility point of view which can be understood as follows:

The ionic conductivity in solid electrolytes is often interpreted in terms of hopping of mobile charge carriers from site to site (Kimball and Adams 1978; Dieterich 1988). For this not only is nearby vacancy needed but also the lattice should be sufficiently open so that the ion can jump from the filled site to the available nearby vacant site resulting in a net mass transport. The conductivity due to such hopping of ions (migration) (Linford and Hackwood 1981), following Nerst–Einstein equation, is

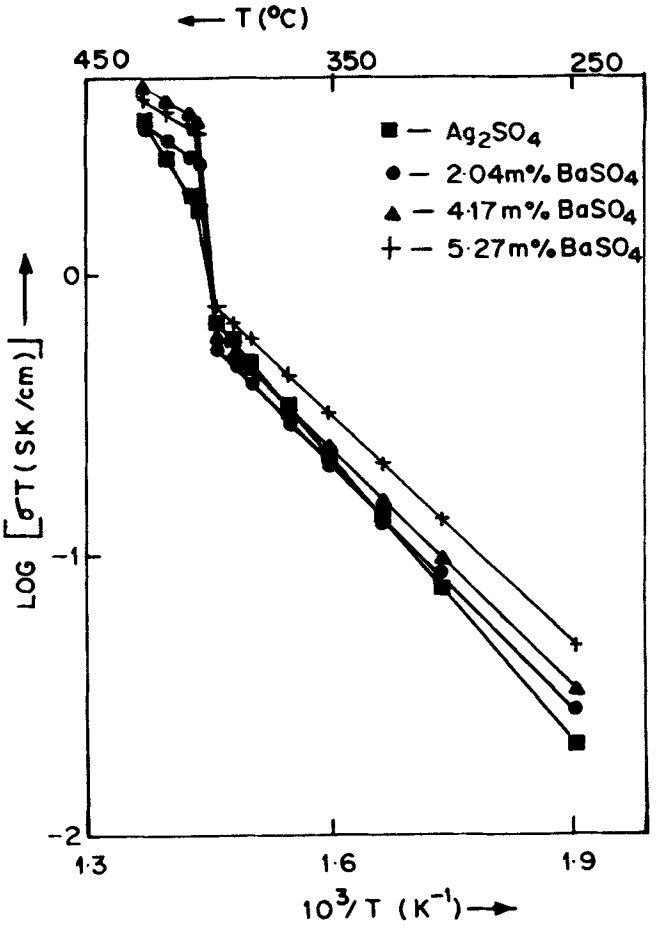

Figure 3. Variation of $\log(\sigma T)$ with $10^3/T$ in $(1-x)Ag_2SO_4$–$(x)BaSO_4$ ($0 \leqslant x \leqslant 0{\cdot}0527$, Region I).

generally expressed as

$$\sigma T = (\sigma T)_0 \exp(-E_a/kT), \tag{1}$$

where $E_a = E_f + E_m$, E_f and E_m are the energy of defect formation and migration respectively, and $(\sigma T)_0$ is a pre-exponential factor. Evidently, the activation energy then is indeed a better criterion for characterization of ionic conductors than the conductivity itself.

The activation energy, E_a, obtained using (1) is found to decrease initially with rise in $BaSO_4$, indicating reduction in E_m. Owing to increase in vacancies along with lattice expansion caused, a large number of ion-percolative pathways are created, thereby enhancing the Ag^+ hopping probability from a filled site to the next available vacant site leading to a net ionic transport.

In the simplest case, the above process can also be visualized by considering the host matrix of pure Ag_2SO_4 (figure 4a) and the modified lattice when the guest Ba^{2+} is partially substituted randomly for Ag^+ (figure 4c). In order to attain the thermodynamical equilibria (constancy of electrochemical potential, constancy of activity and hence a constancy of electric potential) in the vicinity of Ba^{2+}, (i) additional vacancy is created and (ii) expansion of the host lattice takes place, since Ag^+ (1·26 Å) has a much smaller ionic radius than Ba^{2+} (1·38 Å). The disorder reaction using Kröger–Vink notations can be written as

$$\text{I. } Ag_{Ag}(Ag_2SO_4) + x\text{Bä} = (1-x)Ag_{Ag}(Ag_2SO_4) + x[Ba_{Ag}(Ag_2SO_4) + V'_{Ag}(Ag_2SO_4)].$$

The lattice expansion in the vicinity of Ba^{2+} reduces the potential barrier height for nearby mobile Ag^+ ions (figure 4d). Such an additional vacancy with a shallow potential well offers a lower activation energy of migration ($\dot{E}_m$) for mobile Ag^+ which in turn increases the conductivity. The dependence of ionic conductivity on the ionic size of divalent dopant (at fixed vacancy concentration) in Li_2SO_4 reported earlier supports the above discussed model (Singh and Bhoga 1990).

3.2 *Region II*

The variation of $\log(\sigma T)$ with $10^3/T$ for $BaSO_4$ added Ag_2SO_4 samples (biphase) for compositional range region II is shown in figure 5. The conductivity in this region is seen to be optimized at 20 mole% $BaSO_4$ addition, as seen in figure 2. This enhancement in conductivity could be understood in light of the following: According to dispersed-phase theory for MX/M'X, there is a net transfer of cations from either phase across the interface (Maier 1985; Singh 1993). Two probable Frenkel analogue interface reactions are

$$\text{II. } Ag_{Ag}(Ag_2SO_4) + V_i(BaSO_4) = \dot{Ag}_i(BaSO_4) + V'_{Ag}(Ag_2SO_4),$$

and

$$\text{III. } V_i(Ag_2SO_4) + Ba_{Ba}(BaSO_4) = \text{Bä}_i(Ag_2SO_4) + V''_{Ba}(BaSO_4).$$

The corresponding mass action law takes the form

$$C_v C_i = C_0 \exp[-(\Delta G^0)], \tag{2}$$

where C_v and C_i are the vacancy concentration in one phase and interstitial concentration in the other in contact respectively, ΔG^0 is free enthalpy for reaction, and C_0 is the pre-exponential factor.

If the free energy of reaction II exceeds that of reaction III, it gives rise to additional interstitial Ba^{2+} in Ag_2SO_4 leaving behind equivalent vacancies in the $BaSO_4$ lattice; otherwise the converse is true. Since Ba^{2+} is more electropositive than Ag^+, reaction III is thermodynamically favoured. In addition, as a result of repulsive interaction, Ba^{2+} pushes back the surface Ag^+ into the Ag_2SO_4, thus forbidding reaction II. These two factors enrich the interstitial ion and vacancy concentration forming space charge layers close to the Ag_2SO_4 and $BaSO_4$ surface respectively. The presence of foreign Ba^{2+} in space charge region at Ag_2SO_4 surface also leads to the lattice

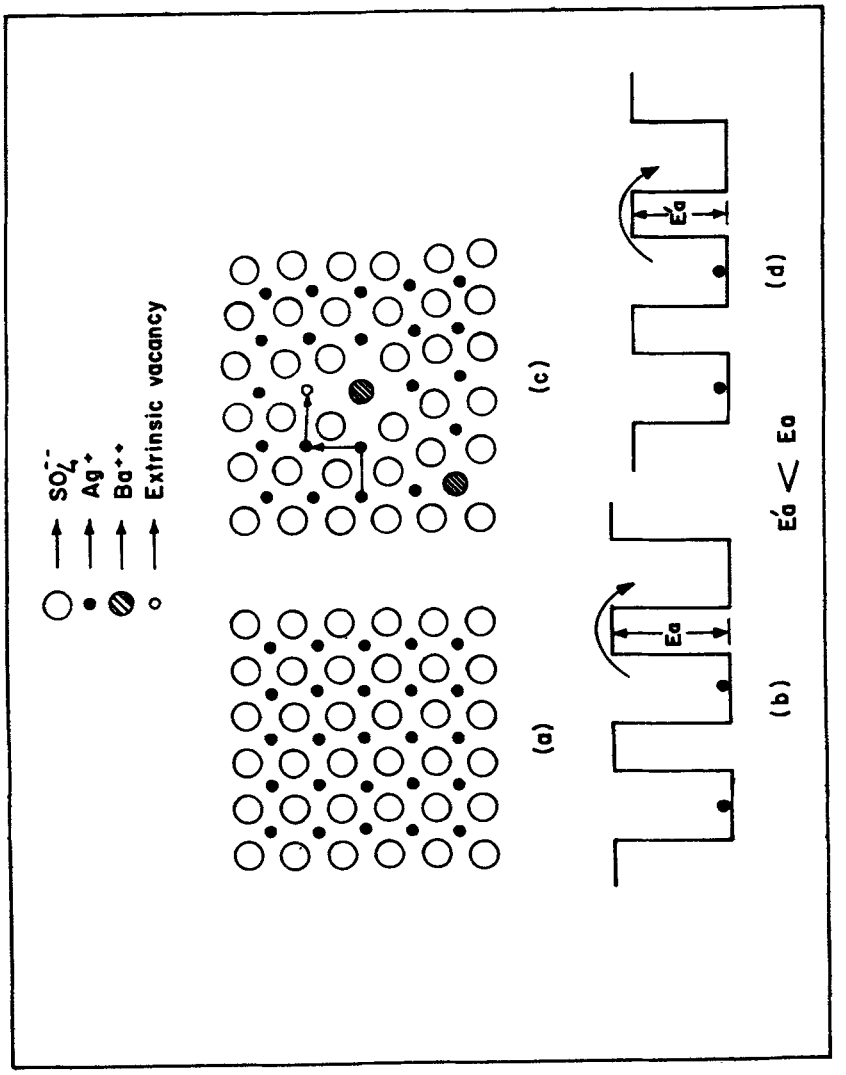

Figure 4. Schematic representation of a Ag_2SO_4 lattice plane through: (**a**) the regular host lattice, (**b**) an ideal potential well, (**c**) the host lattice with some of the Ag^+ partially replaced by Ba^{2+} and (**d**) the modified potential well.

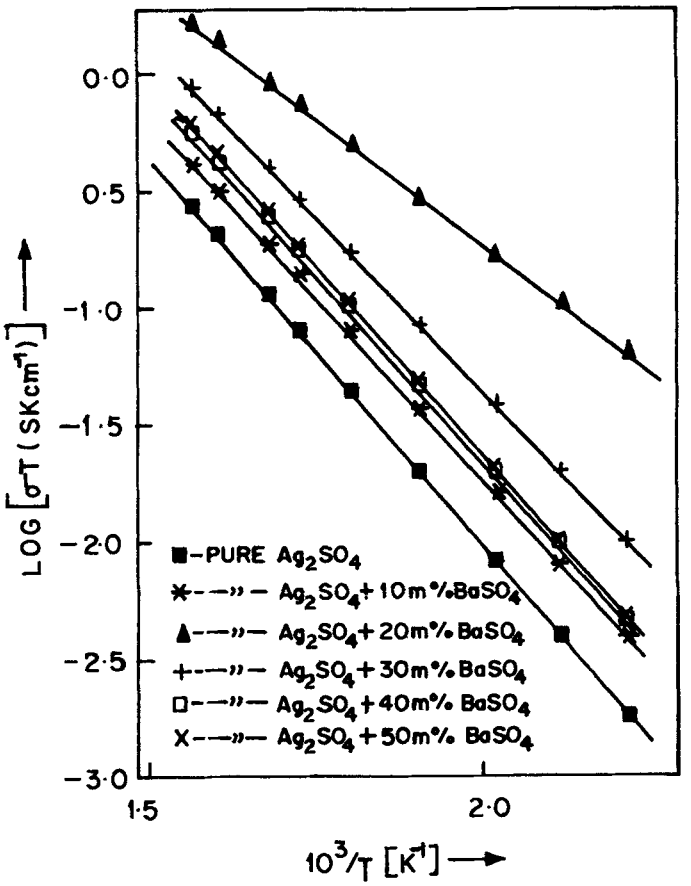

Figure 5. Variation of $\log(\sigma T)$ with $10^3/T$ in $(1-x)Ag_2SO_4$–$(x)BaSO_4(0{\cdot}1 \leqslant x \leqslant 0{\cdot}6)$ in low-temperature phase (Region II).

expansion thus favouring the Ag^+ mobility parallel to the interface which is considered as an ion-percolating path in the space charge region (Bunde *et al* 1985). The maximum conductivity at 20 mole% $BaSO_4$ is due to optimum percolating paths in the sample.

4. Conclusion

Electrical conductivity in $(1-x)Ag_2SO_4$–$(x)BaSO_4(0{\cdot}0 \leqslant x \leqslant 0{\cdot}6)$, characterized by XRD and SEM, has been investigated using complex impedance technique. Partial substitution within the solubility limit (5·27 mole%) of Ag^+ by the bigger Ba^{2+} enhances conductivity in compliance with the classical aliovalent doping theory. A simplistic model based on lattice expansion upon substitution qualitatively accounts for conductivity enhancement. Beyond the solid solubility limit the system behaves as a typical binary composite, with $BaSO_4$ dispersed in Ag_2SO_4. The

enhancement of conductivity upon introduction of excessive $BaSO_4$ into Ag_2SO_4 is reasonably discussed in terms of interfacial reactions and surface-defect chemistry. The percolation threshold seems to occur at 20 mole% $BaSO_4$ resulting in maximum conductivity. Thus both homogeneous and heterogeneous doping of an aliovalent Ba^{2+} ion optimize conductivity in certain compositions which could be considered in electrochemical device applications.

Acknowledgement

Authors are thankful to UGC, New Delhi, for providing financial assistance to carry out this work.

References

Bunde A, Dieterich W and Roman H E 1985 *Phys. Rev. Lett.* **55** 5
Dekker M 1990 *Electrical properties of gas sensor materials*, Ph D thesis, Delft University of Technology, Delft, The Netherlands
Dieterich W 1988 *High conductivity solid ionic conductors* (ed.) T Takahashi (Singapore: World Sc.) p. 17
Gauthier M and Chamberland A 1977 *J. Electrochem. Soc.* **124** 1579
Heed B, Lunden A and Schroeder K 1975 *10th Intersoc. Energy Conv. Eng. Conf. IECEC75 Record* p. 613
Hofer H H, Eysel W and Alpen U V 1981 *J. Solid State Chem.* **36** 365
Kimball J C and Adams L W Jr. 1978 *Phys. Rev.* **B18** 5851
Liang C C 1973 *J. Electrochem. Soc.* **120** 1289
Linford R G and Hackwood S 1981 *Chem. Rev.* **81** 327
Liu Q, Sun X and Wu W 1990 *Solid State Ionics* **40/41** 456
Maier J 1985 *Bur. Bunsenges. Physik. Chem.* **89** 355
Rodger A R, Kuwand I and West A R 1985 *Solid State Ionics* **15** 185
Rao N, Schoonman J and Sorensen O T 1992 *Solid State Ionics* **57** 159
Singh K and Deshpande V K 1982 *Solid State Ionics* **7** 295
Singh K 1988 *Solid State Ionics* **28–30** 1371
Singh K, Chandrayan V R and Deshpande V K 1988 *Solid State Ionics* **27** 57
Singh K and Bhoga S S 1990 *Solid State Ionics* **39** 205
Singh K and Bhoga S S 1992 *J. Solid State Chem.* **97** 141
Singh K 1993 *Solid State Ionics* **66** 5–14
Singh K, Pande S M and Bhoga S S 1995 *J. Solid State Chem.* **116** 232